Global and Planetary Change 243 (2024) 104598

Contents lists available at ScienceDirect

Global and Planetary Change

journal homepage: www.elsevier.com/locate/gloplacha

# Evaluation of nature-based climate solutions for agricultural landscapes in the Galápagos Islands

Ilia Alomía Herrera [a,b,*], Armando Molina [c], Yessenia Montes [b], Jean Louise Dixon [d], Veerle Vanacker [a,*]

[a] Earth and Life Institute, Centre for Earth and Climate Research, Université catholique de Louvain, Louvain-la-Neuve, Belgium
[b] Escuela de Ingeniería Ambiental, Facultad de Ingeniería en Geología, Minas, Petróleos y Ambiental, Universidad Central del Ecuador, Quito, Ecuador
[c] Fundación Terra Ciencia, Cuenca, Ecuador
[d] Department of Earth Sciences, Montana State University, Bozeman, MT, USA

ARTICLE INFO

Editor: Jed O Kaplan

*Keywords:*
Climate change
Global warming
Agricultural drought
Nature-based climate solutions
Silvopasture
Galápagos Islands

ABSTRACT

The Galápagos Islands are highly vulnerable to climate and environmental change, and nature-based solutions can help local communities adapt local agricultural systems. Through a comparative analysis, we evaluated the effects of three land management strategies on soil temperature, soil water availability and storage, and carbon stocks in Santa Cruz Island (Galápagos Archipelago). We installed six monitoring sites that consisted of two replicates per pathway: (i) the avoided loss of tropical forest, (ii) the conservation of scattered trees and living fences in at-risk agroforestry system, and (iii) the increase in biomass after a reduction of the grazing intensity. The monitoring sites were equipped with a dense network of rain gauges, air temperature and relative humidity sensors, and capacitance/frequency probes that registered volumetric water content and soil temperature. After pedological characterization of the soil profiles, the soil physico-chemical and hydrophysical properties were determined in laboratory. Over a period of 30 months (July 2019 to December 2021), hydrometeorological and soil environmental data were collected.

We assessed differences in soil temperature, moisture availability and soil organic carbon content between native forests, sites under traditional agroforestry and under passive restoration. Forest soils were 12 % cooler;, and soil moisture under forest was 20 % higher than in parcels with silvopastural management. Forest soils had a lower dry bulk density, lower saturated hydraulic conductivity and higher water retention capacity in comparison with the other two management types. In silvopastural systems, a decrease of grazing intensity had a positive effect on soil carbon stocks, that were about 50 % higher than in soils under traditional management. This study shows that avoided loss of tropical forest within an agricultural landscape is a promising strategy to mitigate increasing soil temperatures, agricultural drought, and decline in soil organic carbon content. Continued monitoring of the experimental sites is necessary to corroborate the findings of this investigation at longer temporal scales.

## 1. Introduction

The Galápagos Islands like many small islands in the Pacific Ocean face sustainable development challenges. Because of their remoteness, small population, and dependence on natural resources, they are highly vulnerable to climate change impacts (Trueman et al., 2011). Climate impacts include more frequent and intense weather events (such as storms, floods, and heat waves), sea level rise, and ocean warming and acidification. The Galápagos Islands have a small permanent population, of about 25,000 inhabitants but they receive almost 216,000 tourists per year (Instituto Nacional de Estadísticas y Censos, 2015). The economy is highly dependent on tourism, services and fisheries, and in less extent on agriculture (Burbano et al., 2022). Farming is mostly small-scale with 65 % of the farms having less than 5 ha of land that is used for cattle grazing, and in less extent for cultivation of permanent crops, vegetables and fruit (Alomia Herrera et al., 2022). Due to limited investment in commercial agriculture and improved technology, local production has become uncompetitive compared to imported products from the

* Corresponding authors.
*E-mail addresses:* imalomia@uce.edu.ec (I. Alomía Herrera), veerle.vanacker@uclouvain.be (V. Vanacker).

https://doi.org/10.1016/j.gloplacha.2024.104598
Received 18 March 2024; Received in revised form 25 August 2024; Accepted 2 October 2024
Available online 4 October 2024

mainland: it is expected that by 2027, 95 % of the agricultural products will be supplied from the mainland if no policies for sustainable agriculture are implemented (Sampedro et al., 2020).

The increasing reliance on food imports makes the islanders particularly vulnerable to exogenous shocks such as pandemics, climate impacts, disruptions of supply chains or food price and supply volatility (Davila et al., 2021). Besides food supply and security risks (Walsh and Mena, 2016), food imports also increase ecological risks that are associated with the arrival of invasive animals and pathogens, and they are more demanding in terms of waste management (González et al., 2008). To address the increased threats to food security in the islands, there is a renewed interest to strengthen local food systems on non-protected land in Santa Cruz, San Cristóbal, Isabela and Floreana Island. An important co-benefit from local agricultural production is the potential to reduce or revert agricultural land abandonment that enables the establishment and propagation of invasive plant species, such as guava and blackberry, that can propagate in neighbouring land parcels (Jäger et al., 2009). The rapid decrease of the endemic daisy tree *Scalesia pedunculata* in invaded plots on Santa Cruz Island (Jäger et al., 2024) illustrates how spreading of invasive plant species negatively affected the regeneration of native and endemic plants including the restricted areas within the national park. This further emphasised the need to monitor the environmental impacts of agricultural land abandonment.

Local agricultural production systems on the Galápagos Islands are concentrated in the humid highlands, and their environmental sustainability is poorly studied. Climate change is already impacting the agricultural sector (Mena et al., 2020) with a 0.6 °C rise of the mean land surface temperature since the early 1980s and an increase in intensity and frequency of El Niño storm events over the last 50 years (Grothe et al., 2020). As a result of climate change, soils are more prone to agricultural drought in the dry season (Sterling et al., 2013), and susceptible to water erosion and mass movements in the wet season (Toohey et al., 2018). In 2023 and 2024, we registered rainfall events with intensities of more than 125 mm per 24 h in the central parts of Santa Cruz Island. They caused surface runoff in the agricultural area, mudflows and flash floods in the ephemeral channels, and flooding downstream (Paltán et al., 2023). Although these events caused major damage to critical transport infrastructure, and residential and commercial buildings, they are poorly documented in scientific literature and not yet studied.

Nature-based solutions (NbS) are key to sustainable agriculture, as they help to protect, sustainably manage or restore agricultural production systems while simultaneously providing human well-being, food security, and biodiversity benefits (Iseman and Miralles-Wilhelm, 2021). Some solutions, so-called nature-based climate solutions (NbCS) directly prioritize climate benefits with the primary motivation to mitigate GHG emissions and remove $CO_2$ from the atmosphere (Buma et al., 2024), and they include a wide range of pathways from protection to improved management to restoration to manipulated systems. Depending on the land use history and the durability of the NbCS pathway, the implementation of NbCS can be a powerful strategy to transform the agricultural sector of the Galápagos Islands towards more sustainable production (Sonneveld et al., 2018).

In this study, we focused on three potential pathways of nature-based climate solutions that are widely implemented in the non-protected area of Santa Cruz Island. The first pathway, the avoided loss of tropical forest, concerns preservation of forest remnants on agricultural land. These remnants of forests are typically located at remote locations, far from the farm house and access routes (Alomia Herrera et al., 2022), and at the margin of the national park. The second and third pathways concern agroforestry practices. We studied existing silvopastural systems that combine woody species (shrubs and trees) and livestock, and characterized them using Hart et al. (2023) conceptual framework for nature-based climate solutions in agroforestry. Pathway 2 concerns the conservation of scattered trees in pastures, and conservation of living fences in at-risk agroforestry system, while pathway 3 corresponds to an increase in biomass after a reduction of the grazing intensity. In 2019, we selected sites for field monitoring, characterized the major soil physicochemical and soil hydraulic properties per site, and then equipped two true replicates per NbCS pathway with soil and weather sensors. The sites have similar soil type, lithology, topography, and climate, but different NbCS pathway which enables us to evaluate air and soil temperature and humidity temporal variations, soil physicochemical properties, and soil C stocks under different natural climate solutions.

## 2. Study area

Santa Cruz Island is located in the central part of the Galápagos Archipelago, and is a 992 $km^2$ shield volcano (Bow, 1979) rising 950 m above sea level (White et al., 1993), that emerged about 2 million years ago (Schwartz, 2014) (Fig. 1). The island has an inverted-plate shape, with gentle slopes (5 to 10°) in the summital part, steep to very steep slopes (15 to 25°) in the middle part, and gentle slopes (2°) in the basal parts (McBirney and Williams, 1969; Schwartz, 2014). Other remarkable topographic features are the steep volcanic cinder cones, large pit craters (of more than 100 m diameter and 100 m depth) and deeply incised ephemeral or permanent river channels (Schwartz, 2014). The oscillation of the ITCZ provides the archipelago with temperate weather characterized by a hot wet season between January and May with sporadic but intense precipitation and a cool "garúa" season between June and December with persistent cloud cover and frequent drizzle in the uplands (Trueman and d'Ozouville, 2010). In Charles Darwin station (2 m a.s.l.), temperatures of 23–32 °C are recorded in the hot season and 20–25 °C in the "garúa" season. On the windward slope of Santa Cruz Island, there exist strong rainfall gradients during the hot and cold seasons, with mean annual rainfall amounts of less than 300 mm at 2 m a.s.l. in the coastal lowlands and more than 1600 mm in the central highlands (Alomia Herrera et al., 2022 based on Trueman and d'Ozouville, 2010). A lapse rate of −0.8 °C per 100 m elevation is observed (Trueman and d'Ozouville, 2010): the median annual temperature ranges from 23 °C to 25 °C at 2 m a.s.l. at the Charles Darwin Research Station and decreases to 18 °C to 21 °C in the highlands.The inter-annual variation in rainfall can be substantial due to El Nino Southern Oscillations events (Mena et al., 2020; Paltán et al., 2021).

Soils developed on volcanic parent material (Lasso and Espinosa, 2018), and soil properties are controlled by regional hydroclimatic conditions that vary with altitude, orientation, and vegetation cover (Adelinet et al., 2008; Paque et al., 2024; Rial et al., 2017; Taboada et al., 2016). Laruelle and Stoops (1967) and Stoops (2014) defined three distinct pedological units on basalt flows: well-developed Andisols in the very humid and humid highlands, Inceptisols and Alfisols in the transitional wet and warm zones, and slightly weathered Entisols in the arid zones. The soil organic carbon content in the topsoil varies strongly with SOC content of 0.7 % in the arid coastal plain to more than 18 % in the humid highlands (Rial et al., 2017). Similarly large variations are observed in soil hydraulic conductivity ranging from 6.1 mm $h^{-1}$ to 61 mm $h^{-1}$ in the highlands of Santa Cruz island (Adelinet et al., 2008).

More than 88 % of the terrestrial area of Santa Cruz Island is protected since 1959, and part of Galápagos National Park. The remaining area that is mostly located in central and windward side of the island was intended for agricultural activities so that a self-sufficient rural community could establish and develop. In 1961, only 500 inhabitants lived on Santa Cruz Island (Black, 1973) and only 6 % of the non-protected area was used for agriculture, and the remaining part was covered by native vegetation. Agricultural expansion was prominent in the 1960s and 1970s and created an anthropogenic rural landscape as shown in (Alomia Herrera et al., 2022). From the 1990s onwards, the surge of alternative income opportunities in tourism and travel-related services reduced the pressure on the agricultural land. In 2018, forest remnants were preserved on 7 % of the non-protected area, and more than 75 % of the remaining land was under agroforestry (Alomia

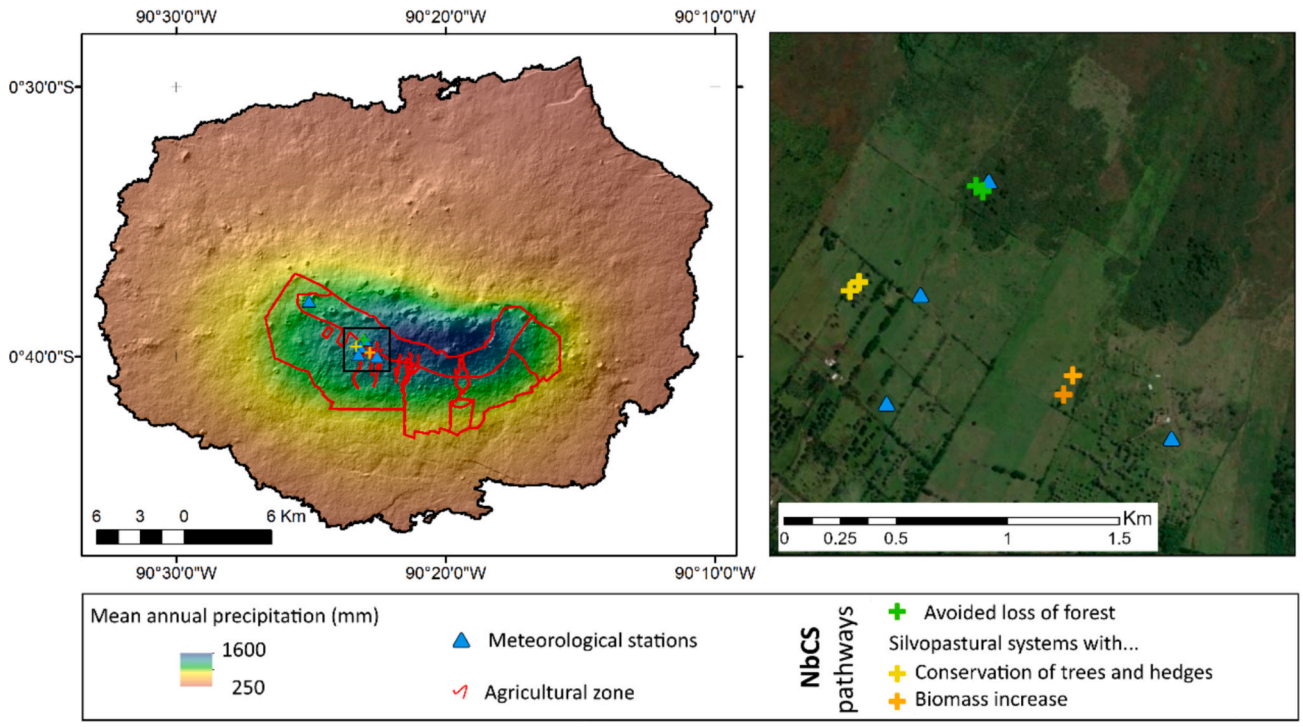


**Fig. 1.** Location of the six study sites in the central part of Santa Cruz Island (Galápagos Archipelago). Three pathways of nature-based climate solutions were monitored: sites with (i) avoided loss of tropical forest, (ii) conservation of scattered trees and living fences in at-risk agroforestry system, and (iii) biomass increase after a reduction of grazing intensity.

Herrera et al., 2022). Silvopastural systems are most common, but there is a wide of variety of management practices adopted by the farmers. While some farmers removed scattered trees and hedgerows on grazing lands, others reduced the grazing intensity which facilitated an increase of shrubs and trees (Jäger et al., 2009; Sampedro et al., 2020).

## 3. Materials and methods

### 3.1. Soil sampling

In order to identify the most appropriate sites for a pairwise comparison of three pathways of nature-based climate solutions, a preliminary soil survey was done in the non-protected area of Santa Cruz Island to identify major variations in soil type, soil depth and structure. After having surveyed more than 120 sites in the agricultural area, we selected study sites in Santa Rosa that are located on the same basaltic sheet flow with similar parent material composition and age. The underlying parent material was dated by $^{40}Ar/^{39}Ar$ geochronology on an ARGUS VI multi-collector noble gas mass spectrometer at Oregon State University following the methods described in Fox et al. (2021) and Schwartz et al. (2022). All sites are located on topographical convexities with low slope gradients without clear evidence of physical erosion or deposition, and have slope gradients between 2 and 8 %. As the sites are located within a 1 $km^2$ area, there is only minimal spatial variation in meteorological conditions. As we controlled for confounding variation from topographic effects, parent material composition and age, and climate, we can evaluate air and soil temperature and humidity temporal variations, soil physicochemical properties, and soil C stocks under three pathways of nature-based climate solutions: (i) the avoided loss of tropical forest, (ii) the conservation of scattered trees and living fences in at-risk agroforestry system, and (iii) the increase in biomass after a reduction of the grazing intensity.

For each NbCS pathway, two true replicate sites were selected on a land parcel with similar management practices (Fig. 1). The replicates are located at approximately 25 to 40 m distance from each other, and all sites were fully equipped and monitored to verify reproducibility of the results. Soil pits (1.2 by 1.2 m) were excavated to the unconsolidated (regolith) layer that overlies the bedrock, reaching depths of 50 to 85 cm. Soil type, depth, texture, colour, consistency, porosity, root depth, and structure of each horizon were described following the USDA guidelines (USDA, 2014). Approximately 1 kg of bulk soil was collected per pedogenic horizon for analysis of grain size, and soil organic carbon content, and several fresh bedrock fragments were collected within the regolith zone for physicochemical analyses and $^{40}Ar/^{39}Ar$ dating. A separate set of undisturbed soil cores was taken with a soil core sampler for the determination of bulk density and hydrophysical properties, with three replicate samples per horizon. The samples were stored cool (4 °C) for further analysis following the procedure described in Carter and Gregorich (2007).

### 3.2. Hydrometeorological data collection

An automatic weather station (HOBO U30 weather station NRC, located at 455 m a.s.l. in pasture) records rainfall, air temperature and relative humidity, incoming solar radiation and wind speed. To exclude potential field-scale variability in meteorology, we also measure rainfall (Rainwise 2.0), air temperature and relative humidity (HOBO U23–002) at three other sites (P420, P450, and P500), respectively in the two types of silvopastural systems and in the site with forest remnants (Table 1, Fig. 2). The weather station, three rain gauges and three air temperature/relative humidity sensors were installed in 2019 following the WMO guidelines, and are logging data since 2019 at 15 min intervals (World Metereological Organization WMO, 2018). In addition, eight capitance/frequency-domain probes were installed at 50 cm depth to track soil temperature, electrical conductivity and volumetric water content variations for the three NbCS pathways. The METER TEROS 12 probes were installed at all six sites at 1 m distance upslope of the soil pits and were inserted at 50 cm depth. In two sites (FOR2 and ABAN1), an extra sensor was installed at 2 m distance from the first sensor for internal cross-validation of the data. All soil sensors were connected to

**Table 1**
Hydrometeorological sensors installed in the experimental sites, with indication of start of the measurements.

| NbCS pathway | Sensor type | code | Type of sensor | Start of measurement |
|---|---|---|---|---|
| Avoided loss of forest | Frequency capacitance probe | FOR1 | Meter TEROS12 | 13/09/2019 |
| | Frequency capacitance probe | FOR21 | Meter TEROS12 | 13/09/2019 |
| | Frequency capacitance probe | FOR22 | Meter TEROS12 | 30/12/2019 |
| | Tipping-bucket rain gauge | P500 | Rainwise | 28/06/2019 |
| | Temperature and rel. humidity | TH500 | HOBO U23–002 | 04/07/2019 |
| Silvopastural system with biomass increase | Frequency capacitance probe | ABAN11 | Meter TEROS12 | 13/09/2019 |
| | Frequency capacitance probe | ABAN12 | Meter TEROS12 | 29/12/2019 |
| | Frequency capacitance probe | ABAN2 | Meter TEROS12 | 13/09/2019 |
| | Tipping-bucket rain gauge | P420 | Rainwise | 28/06/2019 |
| | Temperature and rel. humidity | TH420 | HOBO U23–002 | 04/07/2019 |
| Silvopastural system with conservation of trees | Frequency capacitance probe | AGRI1 | Meter TEROS12 | 13/09/2019 |
| | Frequency capacitance probe | AGRI2 | Meter TEROS12 | 13/09/2019 |
| | Weather station | P450 | HOBO U30 | 28/06/2019 |

EM50 and/or ZL6 dataloggers and are logging data since 2019 at 15 min intervals. The hydrometeorological data were aggregated to daily and monthly values for further analysis.

### 3.3. Determination of soil chemical and hydrophysical properties

The bulk soil samples were air dried and passed through a 2 mm sieve to obtain the fine fraction for laboratory analysis, and the coarse soil fraction content (> 2 mm) was determined by weight. Soil texture of the fine fraction was determined by the laser diffraction particle size analyser (LS 13320, Beckman Coulter). The preparation of samples for texture analysis consisted of grinding a subsample of the fine earth fraction, removal of carbonates with 10 % hydrochloric acid (HCl) and organic matter with 35 % hydrogen peroxide ($H_2O_2$). Before analysis, the samples were treated with ultrasonic to disperse clays. The texture is expressed as a percent of the bulk soil (%) and is classified as sand (63 to 2000 μm), silt (2 to 63 μm) and clay (< 2 μm).

The hydrophysical soil properties were determined on undisturbed soil samples (100 $cm^3$) that were taken in triplicate per genetic horizon. The saturated hydraulic conductivity (Ksat, mm $h^{-1}$) was determined with a permeameter using the constant head method, and results are presented as the mean (and 1 standard deviation) of three measurements. The soil water retention was determined on undisturbed 100 $cm^3$ samples using a sandbox setup for the wettest part of the potential force (pF)-curve, and pressure plate extractors with ceramic plates for pF values between 2 and 4.2. Samples were placed in the sandbox on a kaolin/sand mixture substrate, serving as a medium between the water column and the samples. Suction was then applied to the presaturated samples using a hanging column of water of 1, 3, 10, 31 and 70 cm causing the samples to lose moisture. In the pressure plate extractors, the samples were placed on porous ceramic plates, and pressure was applied. The pressure gradient desaturated the sample until an equilibrium is reached. The measurements in the low-pressure pan were realized at pressures of 0.1, 0.3 and 1 bar. For the measurements at high pressure of 15 bar, composite samples were used. At all steps, the samples were weighted to obtain the gravimetric water content at equilibrium.

All samples from the low-pressure pan were weighed and then placed in the oven at 80 °C for 48 h, as suggested for soils with soil organic carbon content >5 %. Oven-dried samples were again weighed to calculate the dry bulk density, BD, expressed in g $cm^{-3}$, and to convert the gravimetric into volumetric water content (VWC). We reported the values of water retention as the VWC ($m^3m^{-3}$) for a given matric potential ψm (kPa), which is expressed as pF values, where $pF_j = \log10$


**Fig. 2.** View on the sites where the field equipment was installed. (A). Weather station located in the middle of the study area in a silvopasture system (P450). (B). Pluviometer and air temperature/relative humidity probes installed in the at-risk silvopastural system with conservation of trees and living fences (P420) and (C). View on the vegetation in the forest remnants where the soil frequency capacitance probes (METER TEROS12) are installed at 50 cm depth in the forest soil (FOR1).

($-\psi m_j$). We then derived the water retention at saturation at pF = 0 (SAT), field capacity at pF = 2 (FC), and wilting point at pF = 4.18 (WP), as well as the total available water (TAW, m). The latter is calculated by multiplying the difference in soil water content between field capacity and wilting point by the depth of the horizon (m). The supplementary material 2 contains the results of the pF analyses.

### 3.4. Determination of soil organic carbon

Soil organic carbon (SOC, %) was determined on 2 mm sieved dry soil samples by dry combustion with an Elementar Variomax analyser (<0.1 % precision). The total stock in soil organic carbon (SOCstock, Mg $ha^{-1}$) was derived based on Poeplau et al. (2017):

$$SOCstock = \sum_{i=1}^{n} SOC_i \times BD_i \times D_i(1 - RF_i)$$

where $SOC_i$ is the soil organic carbon (mg $g^{-1}$), $BD_i$ is the dry bulk density (g $cm^{-3}$), $D_i$ is soil depth (cm), and RFi is the rock fragment content (%) of soil horizon i. Given that soil thickness varied between sites, we normalized the values to equivalent soil depths of 1 m, and then applied conversion factors to express the SOCstock in Mg $ha^{-1}$.

### 3.5. Data quality control and statistical analysis

To corroborate the coherence of the meteorological and soil physical data, standard data quality assurance and control procedures were applied including preliminary data exploration and processing addressing issues with time formatting and data compilation, detection and flagging of duplicates, outliers and bad (extreme) data using cross-validation techniques with complementary data, and then quantification of eventual data gaps, and the development of complete time series. The data were then formatted to be analysed in R 4.2.2 Software (R Core Team, 2022).

To evaluate the reproducibility of the data, we first tested whether the replicate sites are similar in terms of soil temperature, water availability and storage, and soil hydrophysical properties. For the evaluation of the soil hydrophysical properties, we grouped the samples per genetic horizon. We used the Dplyr and Stats package (R Core Team, 2022; Wickham et al., 2019). Given that replicate measurements were statistically similar ($p < 0.05$), we then evaluated potential differences in the time series of soil surface temperature, and soil water content and availability for plants between different NbCS pathways. We also tested for differences in soil water availability and storage, and bulk density between sites using one-way analysis of variance (ANOVA). *P*-values were estimated using the Bonferroni correction in the kruskal.test function of the "PMCMRplus 1.9.4" package (Pohlert, 2021). As the *p*-values showed heterogeneity of means, the Dunn's post-hoc all-pairs comparison test was applied. Possible dependence of the soil water content and availability on soil physical properties was studied with Pearson's correlation analyses using the function corr in the "Corrplot package 0.92" (Taiyun and Simko, 2021).

## 4. Results

### 4.1. Meteorology of the study area

Over the 30-month period from June 2019 to December 2021, the mean annual rainfall was 1291 mm in P420, 1552 mm in P450, and 1485 mm in P500 over a 1 $km^2$ area, showing a 18 % difference between sites. There is a strong seasonal pattern in rainfall, with January, February, and March recording the highest rainfall amounts and May the lowest. Rainfall during the "garua" season (June to December) ranged from 52 mm to 120 mm per month, which coincides with the months with lower-than-average air temperatures (Fig. 3). Mean annual air temperature ranged between 19.9 and 20.4 °C and shows very little local variation over the 1 $km^2$ study area. However, there is considerable seasonal variation, with March having the highest mean monthly temperature and May the highest daily temperature. Relative humidity remained consistently high and only decreased below 50 % shortly after the rainy season. The most prominent wind directions are South and South-East.

### 4.2. Soil profile description and key soil properties

Soils developed on basaltic parent material, with $^{40}Ar/^{39}Ar$ ages of 84.0 ± 24.1 ka, 94.4 ± 13.8 ka, and 108.6 ± 31.0 ka (Supplementary material 1, reported as mean ± 2 sigma full external error). Based on the numerical age control and the overall geomorphic setting of the study area, we are ascertained that the soils developed on basalt flows of similar age and, hence, composition. The ages of the basaltic flows are consistent with the $^{40}Ar/^{39}Ar$ ages for the Shield Series' basalts reported by Candra et al. (2021), Schwartz et al. (2022) and Paque et al. (2024).

Soils were classified as Andisols, and soils are generally thin as the depth to the C horizon ranged from 43 to 80 cm. There is some local variability in soil depth, with slightly deeper soils (i.e., 70 to 80 cm) in the western part of the study area where the parcels with silvopasture with conservation of scattered trees and living fences are located, and shallower soils (i.e., 45 to 60 cm) in the eastern part in parcels under native forest or silvopasture with reduction of grazing intensity. The effective root depth is 80 to 110 cm in the area (Table 2), and roots penetrate in the weathered parent material. The effective root depth

**Table 2**
Main soil properties (colour, structure and consistency), granulometry of the fine fraction and soil organic carbon content.

| Soil profile | Root depth | Soil horizon | Depth | Colour | Structure | Clay | Silt | Sand | Soil texture | Organic carbon |
|---|---|---|---|---|---|---|---|---|---|---|
| | (cm) | | (cm) | | | (%) | (%) | (%) | | (%) |
| FOR1 | 45 | A1 | 0–12 | 5YR4/2 | moderately thin granular crumb | 36.4 | 63.5 | <0.1 | silty clay loam | 10.3 |
| | | CA | 12–40 | 7.5 YR 3/2 | structureless thin massive | 28.9 | 70.3 | 0.7 | silt loam | 5.6 |
| | | C | 45–55 | 5YR 3/2 | moderately thin granular crumb | 18.2 | 73.9 | 7.8 | silty clay loam | 4.8 |
| FOR2 | 40 | A | 3–15 | 7.5 YR 4/2 | structureless thin massive | 46.8 | 53.2 | <0.1 | silty clay | 10.8 |
| | | C1 | 14–45 | 5YR 3/2 | moderately thin granular crumb | 30.2 | 69.3 | 0.5 | silty clay loam | 4.6 |
| ABAN1 | 40 | A | 12–25 | 7.5 YR 4/2 | structureless thin massive | 39.8 | 60.2 | <0.1 | silty clay loam | 6.9 |
| | | C1 | 25–60 | 5YR4/2 | moderate medium granular crumb | 36.4 | 63.1 | 0.5 | silty clay loam | 3.1 |
| ABAN2 | 46 | A | 1–15 | 7.5 YR 4/2 | moderate thin granular crumb | 41.2 | 58.9 | <0.1 | silty clay | 10.1 |
| | | C1 | 15–50 | 7.5 YR 3/4 | weak thin granular | 39.8 | 60.2 | <0.1 | silty clay loam | 4.8 |
| AGRI1 | 110 | A1 | 3–30 | 5YR4/2 | moderate medium granular crumb | 32.5 | 67.1 | 0.4 | silty clay loam | 4.2 |
| | | A2 | 30–55 | 7.5 YR 4/2 | moderate thin granular crumb | 18.2 | 64.0 | 17.8 | silt loam | 1.5 |
| | | AC | 55–70 | 7.5 YR 3/4 | weak thin granular | 17.8 | 58.0 | 24.2 | silt loam | 0.9 |
| AGRI2 | 80 | A1 | 3–18 | 5YR3/3 | moderately thin granular crumbs | 36.7 | 63.3 | <0.1 | silty clay loam | 6.2 |
| | | A2 | 18–65 | 7.5 YR 4/2 | weak, very thin massive | 29.1 | 65.5 | 5.3 | silty clay loam | 1.9 |
| | | AC | 65–80 | 7.5 YR 4/2 | weak very thin massive | 38.3 | 61.6 | 0.1 | silty clay loam | 1.9 |

follows the same variation as the soil depth. The soils displayed distinctive horizons with contrasting colours: The A horizons were characterized by a dark brownish colour, and abruptly separated from and in sharp contrast to the underlying horizons that exhibited light-colored (e. g., light brownish or yellowish) subsoil or saprolite material that is intensely weathered (Fig. 4). Soil texture analyses show high loam (53.4 to 73.9 %) and clay (17.8 to 46.8 %) fractions, and a very low sand fraction (< 7.8 %, Table 2).

Soil temperature.

Soil temperatures (at 50 cm depth) of all monitoring sites in silvopastural systems (pathway 2 and 3) were similar, with no significant differences in soil temperatures between the two management practices (ANOVA followed by Dunn's post-hoc all-pair comparison, $p > 0.05$). The mean annual soil temperature in these sites was 22 °C, which is about 12 % higher than the mean annual air temperature (Fig. 5A, B & D). Over the year, soil temperatures under silvopastural management varied between 20 °C and 25 °C. In contrast, soil temperatures under forest remnants (pathway 1) were significantly lower than under silvopastural management and ranged between 17 °C and 23 °C (Fig. 5). In the forest soils, the median annual soil temperature at 50 cm depth was very close to the median annual air temperature (i.e., 21 °C) and 3 % higher than the mean air temperature.

The ratio of soil/air temperature is a measure of heat transport in the soil. When the soil/air temperature ratio is higher than the unit, this means that the soil temperature is higher than the air temperature. The parcels under silvopastural management were first taken into cultivation in the 1960s when farmers converted native forest to cropland and, later on, pasture. In these sites, the ratio of soil to air temperature fluctuated between 0.69 and 1.51, with a mean value of 1.14. In the area where native forest is conserved, the soil to air temperature varied between 0.77 and 1.68 throughout the year, with a mean value of 1.03 (Fig. 5E).

Temporal variations in air and soil temperatures at 50 cm depth showed a nearly sinusoidal seasonal pattern with superimposed short-term fluctuations (Fig. 6). Short-term variations are clearly visible in the data collected at 15 min interval (Fig. 6D) with soil/air temperature variations of 0.70 to 1.65 due to strong daily variations in air temperature. When aggregating data at daily time step (Fig. 6E), the seasonal trends become visible with ratios fluctuating between 0.90 and 1.36. Relative daily warming of the soil is strongest during the cooler months of the "garua" season (July to November), and the soil/air temperature ratio oscillated between 1.09 and 1.36 in the silvopastural systems and between 0.98 and 1.19 in the forest remnants. During the warmer season, the daily warming of the soil is lower, and the soil/air temperature ratios oscillated between 0.98 and 1.13 in silvopastural systems and between 0.90 and 1.07 under forest. Fig. 6A illustrates that daily mean soil temperature under the forest remnants stayed below the daily mean air temperature at the start of the warmer season. Counterintuitively, soil warming is lowest during the months with highest solar radiation (Fig. 6E) and lowest relative humidity (Fig. 3), and this can be explained by strong variations in air temperature over the day with cooling of the air during the night and warming during the day.

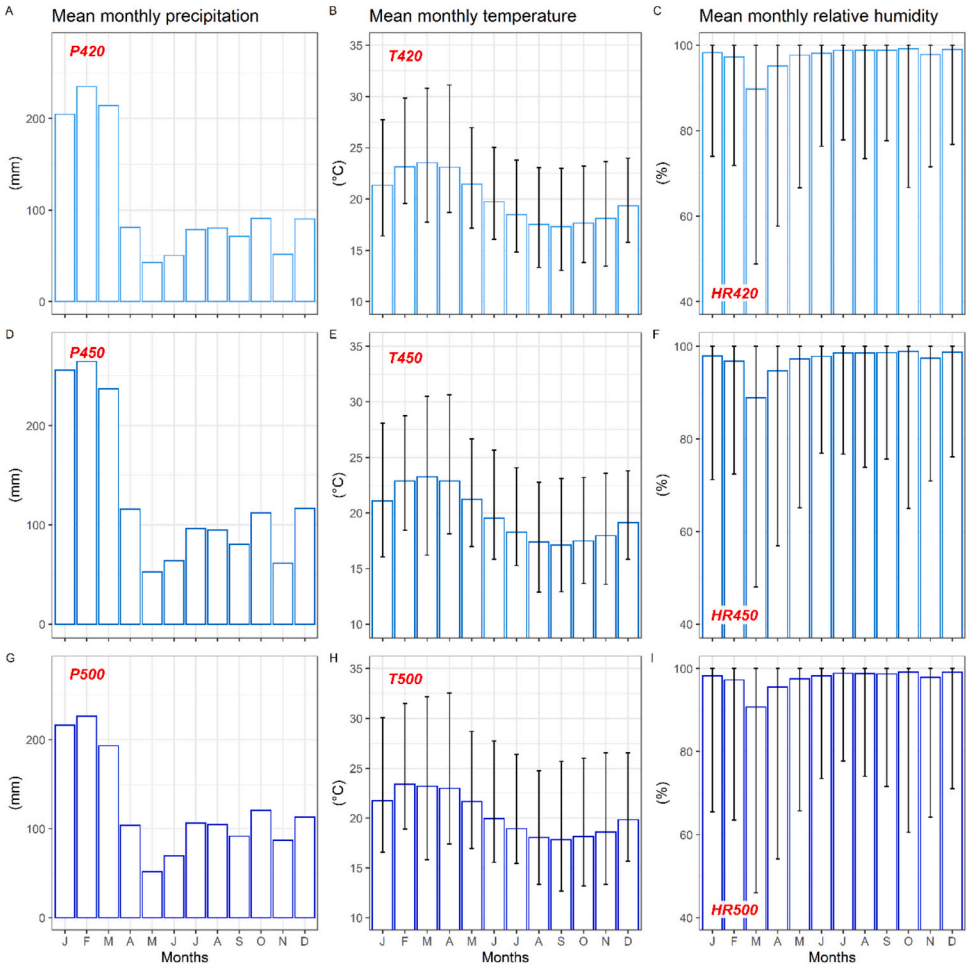


**Fig. 3.** Mean monthly rainfall (mm), air temperature (°C) and relative humidity (%) over the period July 2019 to December 2021 for the stations located at 420, 450 at 500 m altitude. The whiskers represent the minimum and maximum temperature and relative humidity. The location of the weather stations is shown in Fig. 1.

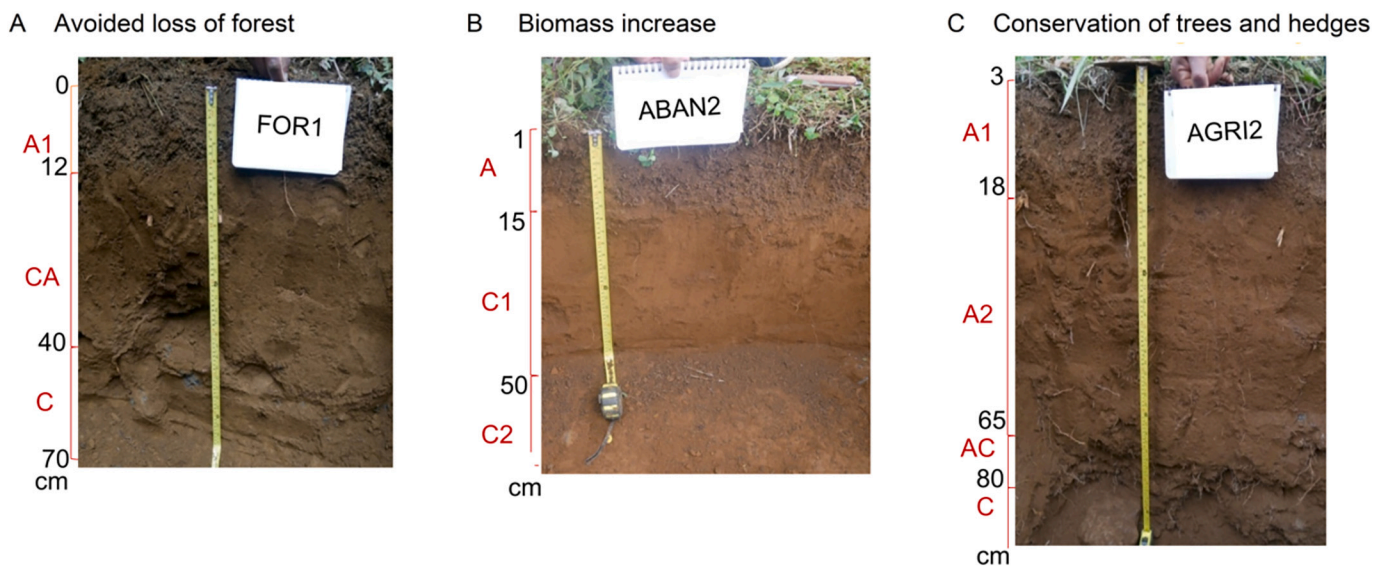


**Fig. 4.** Photographs of three representative soil profiles under forest remnants (left), silvopastural systems with reduction of grazing intensity (middle) and with conservation of trees and living fences (right). The soil horizons are delineated on the left of the pictures, where the soil depths are also marked.

When analysing daily patterns in soil warming (Fig. 6 A-C), it is evident that the soil at 50 cm depth was always warmer than the air during the night hours with soil/air temperature ratios above the unit. Between sunset and sunrise, the air warms faster than the soil and soil/air temperature ratios drop quickly. In sites under silvopasture, the soil temperature is below the air temperature during light hours in the warmer months only (January to April). In sites with native forest, the soil is cooler than the air for 5 to 12 h per day and all year round, illustrating the strong cooling effect of the trees.

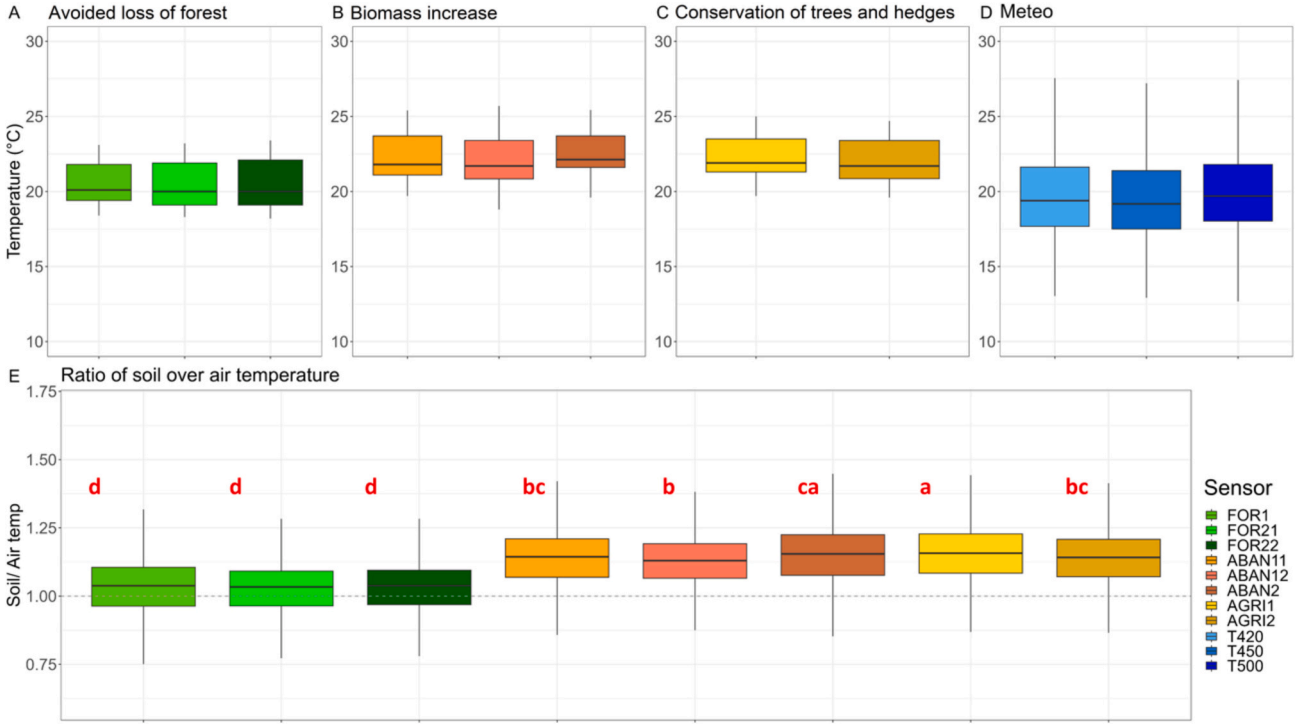


**Fig. 5.** Variation in soil and air temperature (January 2020 – December 2021) between forest conservation, passive restoration and traditional agroforestry. The upper panels (A-D) show soil and air temperature values of the eight soil temperature sensors (at 50 cm depth) and three air temperature probes with the data aggregated at 15-min intervals. The lower panel (E) shows the ratio of the soil to air temperature. The boxes show the median annual value (thick black line) and 25th and 75th percentile, and the whiskers show the interquartile range multiplied by 1.5. The boxplots are colored according to the NbCS pathways with tones of green for the avoided loss of forest (pathway 1), orange for silvopastural land with reduction of grazing intensity (pathway 3) and yellow for silvopastural land with conservation of trees and living fences (pathway 2). Data on air temperature is given in blue tones. Difference between groups was tested with the Kruskal.test function in ANOVA. Groups with a common letter are not significantly different after the Dunn's post-hoc all-pair comparison test at the 5 % level of significance. (For interpretation of the references to colour in this figure legend, the reader is referred to the web version of this article.)

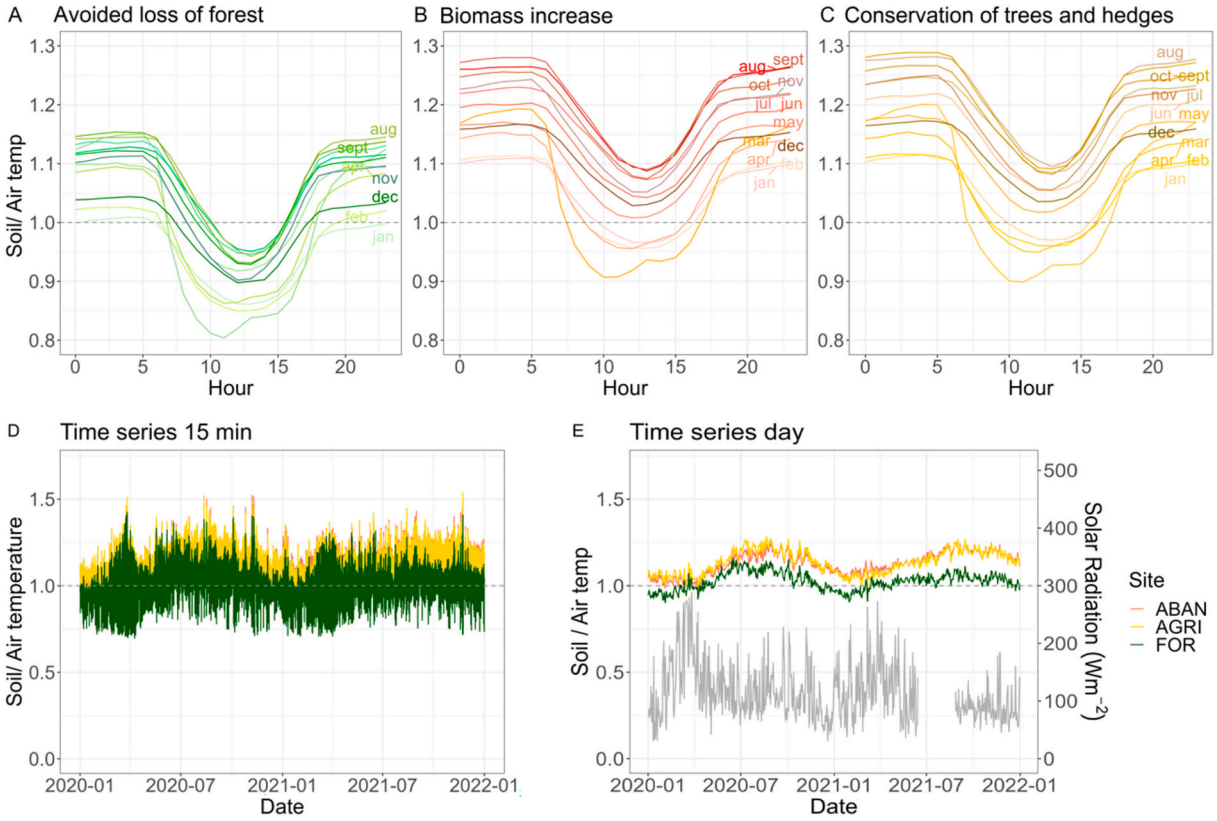


**Fig. 6.** Temporal variation of the ratio of soil to air temperature (January 2020 – December 2021). The upper panels (A-C) show the evolution of the ratio of soil/air temperature over the day, and the values are averaged per month. The lower panels show the soil/air temperature data for the three NbCS pathways, aggregated at 15 min (D) and daily time step (E). The lines are colored according to the management practices with tones of green for the avoided loss of forest (pathway 1), orange for silvopastural land with reduction of grazing intensity (pathway 3) and yellow for silvopastural land with conservation of trees and living fences (pathway 2). Data on solar radiation is plotted in grey. (For interpretation of the references to colour in this figure legend, the reader is referred to the web version of this article.)

### *4.3. Soil hydrophysical properties*

The saturated hydraulic conductivity did not vary between replicates but varied between parcels with different NbCS pathway (Fig. 7A and B). Counterintuitively the lowest Ksat values were measured in the sites with forest conservation, with a Ksat of 98.2 ± 125.3 mm $h^{-1}$ in topsoil and 147.2 ± 143.5 mm $h^{-1}$ in subsoil. The highest hydraulic conductivity was reported in the subsoil of the sites under silvopasture where trees are preserved with a mean Ksat of 1368.2 ± 583.0 mm $h^{-1}$. This stands in strong contrast with the subsoil conductivity in silvopastural sites with reduction of grazing intensity that showed Ksat values of 214.1 ± 241.5 $mmh^{-1}$. Topsoil material under different silvopastural management practices had similar Ksat values, with 384.2 ± 292.4 $mmh^{-1}$ for NbCS pathway 2 and 582.3 ± 265.9 $mmh^{-1}$ for NbCS pathway 3.

Soil compaction did not vary between soil genetic horizons, and the dry bulk density values were highly reproducible between replicate sites (Fig. 7C, Table 3). Soil compaction is lowest in the sites with forest conservation with BD of 0.617 ± 0.072 g $cm^{-3}$ and highest in the sites that were cleared for agriculture. The silvopastural lands had similar soil compaction, as no differences in dry bulk density were observed between parcels under NbCS pathway 2 and 3, with resp. BD of 0.742 ± 0.107 g $cm^{-3}$ and 0.714 ± 0.079 g $cm^{-3}$.

The volumetric water content at a given matric potential is highly reproducible between replicates, and the soil hydro physical data were analysed by soil depth (topsoil vs. subsoil) and NbCS pathway (Fig. 8). In sites with forest conservation, soils have consistently higher volumetric water content, at all matric potential, than soils under silvopastural management. There are differences in the behaviour of top- and subsoil material, especially under forests where topsoil material contains higher volumetric water than subsoil. In the sites under silvopastural practices, the difference in VWC between top- and subsoil is more variable: while the topsoil material for pathway 2 has higher VWCs than for pathway 3, the opposite is observed for subsoil material at low pF values.

At field capacity the topsoil in parcels with forest conservation retains 58 and 46 % more water than the topsoil under silvopastural management under pathway 2 and 3. In the subsoil the difference between forest and the sites that were cleared and now under NbCS pathway 2 and 3 is just 26 % and 25 % respectively. Similarly, at wilting point the topsoil in the forest retain 25 % and 24 % more water in the topsoil than the topsoil under silvopastural management under pathway 2 and 3, and in the subsoil, it is just 12 to 0.1 % respectively. Due to the strong differences in VWC of the soils between field capacity and wilting point, the total available water (TAW) in soils under forest conservation is twice the amount of TAW in sites that were cleared for agriculture and now under silvopastural management practices.

According to the correlation results, the VWC at pF = 0 is higher when there is lower dry bulk density ($r^2 = 0.62$, $p$-value = 0.0005, $n$ = 15), higher soil organic carbon content ($r^2 = 0.48$, $p$-value = 0.0044, $n$ = 15), lower depth ($r^2 = 0.52$, p-value = 0.027, n = 15), lower Ksat ($r^2$ = 0.39, p-value = 0.025, n = 15), lower sand content ($r^2 = 0.38$, $p$-value = 0.014, $n$ = 15), and higher clay content ($r^2 = 0.29$, $p$-value = 0.04, $n$ = 15). The Ksat explains most of the variation of the VWC at field capacity ($r^2 = 0.26$, $p$-value = 0.031, $n$ = 15), but we found no correlation that explains the variation at the wilting point. Overall, the Ksat values decrease when the soil organic carbon content increase ($r^2 = 0.18$, p-value = 0.035, n = 15), increases when sand content increases ($r^2$ = 0.33, p-value = 0.026, n = 15). The Ksat values also increase with depth ($r^2 = 0.81$, p-value = 0.029, n = 15), which is mostly due to the Ksat results in the subsoil of the traditional agroforestry area. In contrast, dry

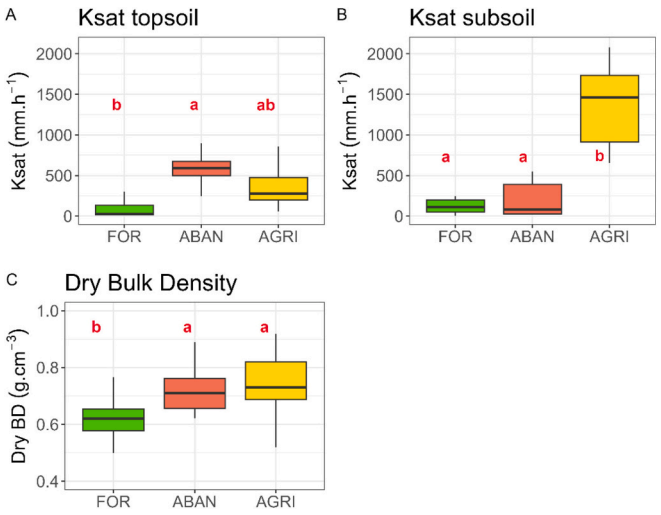


**Fig. 7.** Soil physical properties. (A-B) Saturated hydraulic conductivity (mm. h$^{-1}$) of topsoil (A, A1, A2) and subsoil (AC, CA, C) horizons, analysed per NbCS pathway. (C) BD (g.cm$^{-3}$) of all soil horizons analysed per NbCS pathways. The boxes show the median annual value (thick black line), and the 25th and 75th percentile of the data, and the whiskers show the interquartile range multiplied by 1.5. The boxplots are colored according to the management practices with tones of green for the avoided loss of forest (pathway 1), orange for silvopastural land with reduction of grazing intensity (pathway 3) and yellow for silvopastural land with conservation of trees and living fences (pathway 2). Difference between groups was tested with the Kruskal.test function in ANOVA. Groups with a common letter are not significantly different after the Dunn's post-hoc all-pair comparison test at the 5 % level of significance. (For interpretation of the references to colour in this figure legend, the reader is referred to the web version of this article.)

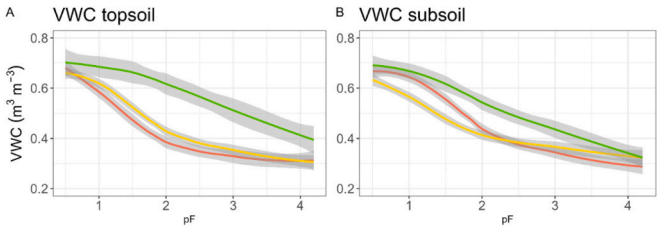


**Fig. 8.** Volumetric water content (VWC) of soils at different pressures. (A) VWC of topsoil (A, A1, A2) material and (B) VWC of subsoil (AC, CA, C) material. The lines are colored according to the management practices with tones of green for the avoided loss of forest (pathway 1), orange for silvopastural land with reduction of grazing intensity (pathway 3) and yellow for silvopastural land with conservation of trees and living fences (pathway 2). The shadow around each line represents the 95 % confidence interval around each trend line. (For interpretation of the references to colour in this figure legend, the reader is referred to the web version of this article.)

bulk density increases with depth ($r^2 = 0.38$, p-value = 0.0024, n = 15). The TAW increases when the Ksat decreases ($r^2 = 0.33$, p-value = 0.02, n = 15).

### 4.4. Carbon content and stocks

Our results point to differences in soil organic carbon content between sites under different NbCS pathways, but our dataset based on two replicates per NbCS pathway does not allow to test for statistical significance. Soil organic carbon content occurs to be higher in sites with forest conservation (4.6 to 10.3 %) and silvopastural lands with reduced grazing intensity (3.1 to 10.1 %) than in silvopastural lands with conservation of trees and living fences (0.9 to 6.2 %) (Fig. 9). Soils in the areas with avoided forest loss have the largest soil organic carbon stocks normalized at 1 m, i.e. 384 Mg C ha$^{-1}$ (Table 3), followed by silvopastural land with biomass increase after reduced grazing (378 Mg C ha$^{-1}$) and followed by silvopastural land with conservation of trees (i.e., 190 Mg C ha$^{-1}$). Topsoil material has – on average – about two times more SOC than subsoil material, and the decline of SOC with depth is largest under silvopastural systems with scattered trees where subsoil material has less than 2 % of SOC.

As expected, the SOC decreases with soil depth in topsoil ($r^2 = 0.65$, p-value =0.02, n = 15), and subsoil ($r^2 = 0.68$, p-value =0.02, n = 15). SOC is negatively related to the dry bulk density in the topsoil ($r^2 = 0.55$, p-value = 0.04, n = 15) with increasing SOC in soils with low compaction. The relationship is less evident in the subsoil ($r^2 = 0.45$, p-value =0.1, n = 15). There is a strong positive correlation between SOC, Ksat and volumetric water content at saturation in the topsoil (for Ksat: $r^2 = 0.07$, p-value =0.52, n = 15; and $VWC_{SAT}$: $r^2 = 0.71$, p-value <0.01, n = 15) and subsoil ($r^2 = 0.83$, p-value <0.01, n = 15).

## 5. Discussion

### 5.1. Forest cover mitigating soil heating

In the study sites in Santa Cruz Island, the mean annual soil temperature in sites where forest is conserved (i.e., 21 °C), was close to the mean annual air temperature, and 1.7 °C lower than the mean annual soil temperature under silvopastural management practices (22 °C). Osman (2013) corroborates that mean annual soil and air temperatures can differ by up to 2 °C due to continuous solar radiation throughout the year in humid tropical regions. In the Galápagos Islands with an equatorial climate, there are strong daily variations in soil warming. Between sunset and sunrise, the air warms faster than the soil, and the soil/air temperature ratios quickly drop. Our data reveal that the soils in forested areas can cool down by as much as 5 °C compared to the surrounding agricultural area, and buffer daily temperature fluctuations, as has been seen in studies in Nigeria (Ghuman and Lal, 1987; Lal and Cummings, 1979), Malaysia (Nuruddin and Tokiman, 2005), Borneo (Hardwick et al., 2015), China (Otsuki et al., 2014) and Brazil (Gomes et al., 2016). (Campbell and Norman, 1998; Mu et al., 2007; Shukla, 2014).

According to the literature, the soil temperature is tightly linked to the proportion of sunlight penetrating the tree canopy and reaching the forest floor and the light interception rate of trees (Zheng et al., 1993). Soils warm less when vegetation has a higher foliage surface: following the Beer-Lambert law, foliage increases both the quantity of solar radiation reflected upwards, and the amount of radiation absorbed by the plant canopy and leads to less radiation that reaches the soil surface (Hardwick et al., 2015). In addition, more exuberant foliage reduces the turbulent mixing of air from above the canopy, thereby reducing the influence of above-canopy temperature on soil temperatures (Otsuki et al., 2014; von Haden et al., 2019). A measure commonly used in soil temperature modelling is the leaf area index; with increasing leaf area index, the protection against the sun rays increases with positive cooling effects on the soil temperature. In the study area, there are large differences in leaf area index between the native forest and pastures: the leaf area index is estimated at 2.7 in degraded or secondary forest stands (Pryet et al., 2012), while it ranges in pastures between 0.7 and 1.3 depending on land management practices (Buck et al., 1999). The large difference in leaf area index explains why soils under conserved forests are better protected against direct solar radiation than soils under silvopastural management.

Meteorological factors can explain the seasonal variation of soil temperatures in the study sites as clouds can absorb and reflect radiation (Shukla, 2014). Over the cooler "garua" season, the continuous presence of thick clouds in the central part of Santa Cruz Island results in the reflection of a significant part of the incoming solar radiation (Trueman and d'Ozouville, 2010). This causes the sunlight to dwindle before reaching the ground and explains why the air and soil had lower

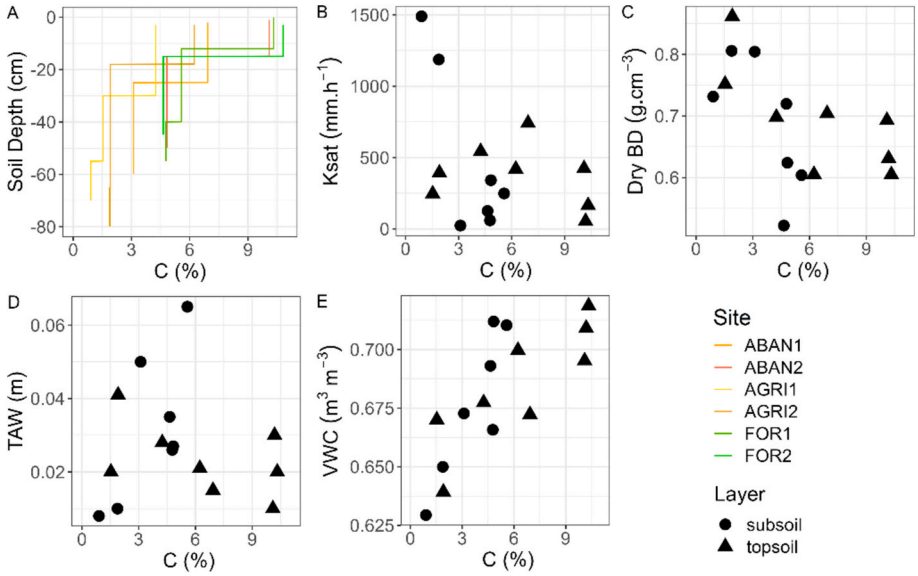


**Fig. 9.** Variation of soil organic carbon (%) with soil depth (panel A), saturated hydraulic conductivity (panel B), dry bulk density (panel C), total available water (panel D), and volumetric water content at saturation point (panel E). The profiles are colored according to the management practices with tones of green for the avoided loss of forest (pathway 1), orange for silvopastural land with reduction of grazing intensity (pathway 3) and yellow for silvopastural land with conservation of trees and living fences (pathway 2). In panel B the topsoil (horizon A, A1 and A2) values are shown with black triangular points and the subsoil (horizon AC, CA, C and C1) values are indicated in black circles. (For interpretation of the references to colour in this figure legend, the reader is referred to the web version of this article.)

**Table 3**
Summary of the hydrophysical characteristics per horizon and per soil profile, with BD, Ksat and volumetric water content at field capacity (pF = 2) and wilting point (pF = 4.18), and total available water. Data are the mean value of three replicates (±1SD).

| Soil profile | Soil horizon | BD | Ksat | VWC at FC | VWC at WP | Total available water | Carbon stocks |
|---|---|---|---|---|---|---|---|
| | | (g cm$^{-3}$) | (mm h$^{-1}$) | (m$^3$ m$^{-3}$) | (m$^3$ m$^{-3}$) | (m) | (Mg C ha$^{-1}$) |
| FOR1 | A1 | 0.605 ± 0.046 | 165.0 ± 196.2 | 0.603 ± 0.122 | 0.398 ± 0.052 | 0.020 ± 0.011 | 400.32 |
| | CA | 0.604 ± 0.027 | 248.4 ± 187.6 | 0.591 ± 0.043 | 0.313 ± 0.033 | 0.065 ± 0.002 | |
| | C | 0.720 ± 0.051 | 60.1 ± 80.3 | 0.561 ± 0.04 | 0.358 ± 0.020 | 0.026 ± 0.008 | |
| FOR2 | A | 0.631 ± 0.017 | 53.7 ± 68.7 | 0.625 ± 0.024 | 0.390 ± 0.021 | 0.030 ± 0.005 | 367.57 |
| | C1 | 0.522 ± 0.020 | 126.0 ± 81.1 | 0.468 ± 0.044 | 0.304 ± 0.073 | 0.035 ± 0.029 | |
| ABAN1 | A | 0.704 ± 0.026 | 741.1 ± 221.8 | 0.384 ± 0.026 | 0.306 ± 0.004 | 0.015 ± 0.005 | 342.34 |
| | C1 | 0.804 ± 0.074 | 23.5 ± 7.4 | 0.450 ± 0.031 | 0.321 ± 0.020 | 0.050 ± 0.001 | |
| ABAN2 | A | 0.693 ± 0.065 | 423.4 ± 248.9 | 0.389 ± 0.039 | 0.319 ± 0.007 | 0.010 ± 0.001 | 412.97 |
| | C1 | 0.624 ± 0.003 | 341.2 ± 236.8 | 0.428 ± 0.007 | 0.291 ± 0.018 | 0.027 ± 0.004 | |
| AGRI1 | A1 | 0.698 ± 0.056 | 543.2 ± 443.2 | 0.454 ± 0.053 | 0.307 ± 0.044 | 0.028 ± 0.001 | 117.13 |
| | A2 | 0.752 ± 0.088 | 245.9 ± 105.9 | 0.391 ± 0.014 | 0.291 ± 0.014 | 0.020 ± 0.006 | |
| | AC | 0.732 ± 0.069 | 1489.3 ± 741.7 | 0.407 ± 0.025 | 0.316 ± 0.029 | 0.008 ± 0.007 | |
| AGRI2 | A1 | 0.606 τ0.084 | 419.5 ± 132.3 | 0.418 ± 0.042 | 0.279 ± 0.006 | 0.021 ± 0.003 | 202.90 |
| | A2 | 0.862 ± 0.051 | 393.0 ± 459.7 | 0.450 ± 0.026 | 0.332 ± 0.011 | 0.041 ± 0.005 | |
| | AC | 0.806 ± 0.112 | 1186.6 ± 386.7 | 0.417 ± 0.042 | 0.330 ± 0.026 | 0.010 ± 0.004 | |

temperatures during cloudy days of the garua season than sunny days with clear sky of the warm season. In addition, oscillations of the intertropical convergence zone (ITCZ) are responsible for changes in marine currents and oceanic winds. During the warm season, the sea surface temperatures are higher than in the garua season (Paltán et al., 2021), and they warm up the air above the ocean. When trade winds reach the island during the warm season, they also transport warm air inland. The opposite pattern occurs when the cold oceanic currents reach the Galápagos Islands in July and August. Therefore, the seasonal temperature pattern is linked to seasonal variations in incoming solar radiation and sea surface temperatures due to changes in marine currents and oceanic winds.

Lastly, soil properties influence soil warming, and the soil thermal regime depends on thermal conductivity, heat capacity, and air and water content (Ochsner, 2019; Osman, 2013). Since water has a higher heat capacity (4.18 J g$^{-1}$ °C$^{-1}$) than basalt rock (0.409–0.68 J g$^{-1}$ °C$^{-1}$) or air (1 J g$^{-1}$ °C$^{-1}$); it takes more energy to warm wet soils than dry soils (Robertson and Peck, 1974). Because of their higher porosity, soils with low bulk density can store more water or air which affects the soil temperature regime. Our results show how the soil moisture regime influences soil temperature (Fig. 5A-C) with abrupt changes in the soil/air temperature ratio during the afternoons in March when storm events are frequent. The sudden change in soil temperature is likely caused by the soothing effect of rainwater penetrating the soil matrix. We observed that the sites under forest were less prone to warming than land parcels under silvopastural management. Besides their higher foliage cover, they also have higher soil porosity and organic carbon content, and higher soil volumetric water content. The cooling effect of forest soils is essential to buffer daily temperature fluctuations and can be crucial to mitigating warming in the context of climate change in the Galápagos Islands.

### 5.2. Forest cover and soil water balance

Previous studies in the Galápagos islands mostly focused on natural variations in soil (hydro)physical properties and analysed soil physico-chemical properties as function of climate and soil development. In the agricultural area in the central part of Santa Cruz Island, Andisols are prevalent according to Laruelle (1966) and Stoops (2014). The unique mineralogical composition and soil organic carbon content of Andisols result in specific physical and mechanical properties, including fluffy consistency, high porosity, low bulk density, and high water retention capacity (Rodríguez Rodríguez et al., 2005). The dry bulk density is often below below 0.90 g $cm^{-3}$ (Sobotkova et al., 2011) and varies with soil organic carbon content and weathering degree (Lal, 2016; Molina et al., 2019). Our analyses show dry bulk densities between 0.50 and 0.90 g $cm^{-3}$, which are in line with earlier observations by Laruelle (1966) and Stoops (2014) who reported dry bulk densities below 0.85 g $cm^{-3}$, and Dinter et al. (2020) who reported values between 0.55 and 0.75 g $cm^{-3}$. Our study shows – for the first time – that land management practices have an impact on physical soil degradation, with soils under pasture (BD = 0.742 ± 0.107 g $cm^{-3}$) having significantly higher bulk density than those under native forests (BD = 0.617 ± 0.072 g $cm^{-3}$). There is no effect of the silvopastural management on soil compaction.

The soil hydraulic conductivity shows large variation, with values of Ksat between 20 and 1500 mm $h^{-1}$ (Table 2). Such large variations in hydraulic conductivity are not uncommon in Andisols, and Páez-Bimos et al. (2022) also reported two-order of magnitude variations in Ksat values in Andisols. We observed the lowest hydraulic conductivities in topsoil and subsoil in sites under forest conservation, with Ksat of 98.2 ± 125.3 mm $h^{-1}$ for topsoil and 147.2 ± 143.5 mm $h^{-1}$ for subsoil, and the highest values of 1489.3 ± 741.7 mm $h^{-1}$ in subsoil of sites under silvopastural management with conservation of scattered trees and living fences. The Ksat values that we obtained under forest are higher than the values that Adelinet et al. (2008) reported for soils under protected forest in the highlands of Santa Cruz (i.e., 6.1–61 mm $h^{-1}$), but this can be due to differences in the methods used to determine the Ksat and/or local variability in soil properties. The soil hydraulic conductivity in soils under conserved forest is systematically lower than under silvopastural management (Fig. 7). We cannot attribute these differences to the overall soil porosity as forest soils have higher overall porosity than sites that were converted to agriculture. However, we pose that the soil structure plays an important role: under natural conditions, Andisols are often structureless with abundance of micropores that reduce water movement compared to well-aggregated soils with macro pores (Shukla, 2014). The parcels that are now under silvopastural management were ploughed in the past when the area was first taken into cultivation (Barrera et al., 2019), and it is known that labour and tillage practices increase the formation of crumbs and macro-porosity (Martins et al., 1991). Infiltration rates between structured and structureless soils can differ significantly, up to tenfold (Kutílek and Nielsen, 2015).

Besides the above-mentioned differences in soil compaction, and hydraulic conductivity, the soils under silvopastural management have lower total available water and lower volumetric water content across all matric potentials than the sites under conserved forest (Fig. 7). At saturation point, the difference between forest soils and those under silvopastural management is only 3 to 5 % and might be due to differences in dry bulk density and soil organic carbon content. With increasing matric potential, the difference in volumetric water content between the sites with avoided loss of forest and the sites under silvopastural management increases, and at wilting point, the water content of the topsoil under forest is 25 % higher than in the other sites. This confirms earlier work in Andisols that showed how forest clearance leads to soil exposure, with changes in clay mineralogy, soil organic carbon content, and soil structure which cause major changes in soil water retention (Cusack et al., 2012; Osher et al., 2003).

### 5.3. Agroforestry and soil carbon stocks

Our preliminary results on soil carbon stocks showed that the lowest soil carbon stocks occur in sites with silvopastural management where only scattered trees and living fences are conserved (pathway 2). In these sites, the SOC content ranges between 6.2 % and 4.2 % for topsoil, and decreases with depth till 1.9 and 0.9 % for subsoil material, and is about 2 times lower than under forest (Fig. 9). In pastures under this type of silvopastural management, the grass biomass is effectively removed by grazing animals, and soils are regularly turned over by ploughing to reseed the pastures. Tillage practices typically lead to the exposure of previously buried organic matter to oxygen, and it is known to increase soil aeration, accelerate microbial decomposition of organic materials, and cause a reduction of SOC stocks over time (Anindita et al., 2022; Koga et al., 2020). The reduction of grazing intensity, that is associated with an increase in the above-ground grass, herbs and shrub biomass, seems to have an impact on SOC content, as our data point to SOC stocks between 10.1 % and 6.2 % for topsoil, and decreases with depth till 4.8 and 3.2 % for subsoil for this type of silvopastural management (i.e., pathway 3 has two times higher SOC stock than pathway 2). The highest SOC stocks are observed in sites with avoided loss of forest, due to high SOC contents in top (~ 10 %) and subsoil (~4.5 %). This is the result of an enhanced input of above-ground biomass from the tree, shrub, herb and grass cover in the conserved forest, and reduced SOC decomposition because of relatively lower soil drainage, higher soil water content, and lower soil temperature (Anindita et al., 2022; Cusack et al., 2012; Koga et al., 2020; Lal, 2016).

Global climate change will result in higher convective precipitation in the Galápagos Islands, and some studies argued that climate change is already causing more distinct seasons in the Galápagos archipelago (Paltán et al., 2021). The rising temperature may enhance decomposition of soil organic carbon and convert the organic-rich Andosols into a source of atmospheric $CO_2$ as biological and chemical transformation of the organic carbon is shown to increase with temperature. In addition, the activity of decomposing microorganisms can also change with temperature and soil water regime leading to quicker depletion of soil organic carbon (Mitchard, 2018). Soil carbon has become a central issue in sustainable agroforestry management practices for its role in mitigating climate change. In the humid agricultural zone in Santa Cruz Island, forest soils contain 2 times more organic carbon than the soils under traditional silvopastural management while in the places where the grazing intensity has diminished the carbon stocks are almost at the same level as in the forest due to biomass accumulation. The presence of forest patches has a positive effect on the soil micro-climate: within forests, the soil temperature is about 2 °C lower than under traditional agroforestry, and the daily temperature fluctuations are strongly buffered. The soils are humid during most of the year, and they store large quantities of water which help to buffer soil warming. Their cooling effect in combination with high soil water content contribute to reduce organic carbon decomposition. Our data point to the importance of silvopastural management on soil organic carbon stocks. A decrease in grazing intensity in silvopastural systems can help to reduce the effect of global warming as this NbCS pathway has positive effects on the soil carbon stocks. However, the impact on soil cooling, soil water balance and total available water content is not confirmed by our results. This points to the importance of long-term monitoring of soil properties under different NbCS pathways, as soil hydrophysical properties might take more time to recover after disturbance.

## 6. Conclusions

In Santa Cruz Island, nature-based climate solutions can contribute to transform the agricultural sector towards more sustainable production. Our data show that soil warming, soil water availability and water content, and carbon stocks differ between land parcels with different management practices. In the at-risk silvopastural systems, where

scattered trees and living fences are conserved, soil compaction is high and water storage capacity is low. Soil carbon stocks are low which might be caused by enhanced soil respiration after ploughing for reseeding grass. Parcels that underwent a reduction of grazing intensity had an increase in grass, herb, and shrub biomass. They were characterized by higher soil carbon stocks and less soil compaction than silvopastural systems without change in grazing intensity. These results are consistent with literature, and point to the importance of managing and monitoring cattle livestock densities in pastures as this can play a role in improving climate resilience within agroforestry systems.

The conservation of patches where forest loss is avoided, has significant impact on the reduction of soil warming, maintenance of soil water content and availability, and soil carbon stocks. Forest patches protect soils against direct solar radiation and keep soils 12 % cooler than in pastures. The protection against soil warming is further enhanced by the soil hydraulic properties of the undisturbed soils that maintain higher soil water content at all matric potentials compared to sites under silvopastural management. Besides their positive effects on soil cooling, water availability, and soil porosity, the forest patches store large quantities of soil organic carbon. The soil microclimate under forest vegetation, with cooler and wetter soils, can help to reduce organic carbon decomposition. As such, conserving forest patches within the non-protected area can help mitigate climate change impacts.

Continued monitoring of the experimental sites is necessary to corroborate the findings of this investigation over longer temporal scales, and an increase of the number of experimental sites will allow to study the effects of NbCS at the landscape scale. Long-term monitoring is crucial to assess the effectiveness of these practices in contributing to climate change mitigation through sustained carbon sequestration, evaluate how these systems respond to severe extreme weather events, such as ENSO, and track the evolution of soil conditions, particularly in terms of soil carbon stocks, bulk density, and water retention capabilities. Long-term data will provide deeper insights into the resilience and sustainability of agroforestry practices and inform adaptive management strategies.

## Funding

This research was facilitated by the Institutional Support Programme of the Académie de Recherche et Education Supérieur de la Fédération Wallonie-Bruxelles (ARES CCD) to the Central University of Ecuador, and funded through the Belgian Development Cooperation. We acknowledge funding from UCLouvain through the Special Research Fund 2019 (FSR) and the Fonds de la Recherche Scientifique FNRS through the FRFC project T.0211.22 granted to Veerle Vanacker.

## CRediT authorship contribution statement

**Ilia Alomía Herrera:** Writing – original draft, Visualization, Funding acquisition, Formal analysis, Data curation, Conceptualization. **Armando Molina:** Writing – review & editing, Methodology, Conceptualization. **Yessenia Montes:** Data curation. **Jean Louise Dixon:** Writing – review & editing, Methodology, Conceptualization. **Veerle Vanacker:** Writing – review & editing, Visualization, Supervision, Methodology, Funding acquisition, Conceptualization.

## Declaration of competing interest

The authors have no competing interests to declare.

## Data availability

The data supporting this study is available at the UCLouvain dataverse at https://doi.org/10.14428/DVN/QAEMIL.

## Acknowledgments

This study was conducted under Research Permit No. PC-98-18, PC-46-19, PC-01-21 and PC-45-22 of the Galápagos National Park, and was only possible with the help of the landowners that allowed us to perform the experiments and the installation of environmental sensors at their farms. We acknowledge the support of Peter Schiess, his daughter Roberta and the Schiess family, and the support of Amanda Espin and the Espin family. We extend our thanks to Richard Rubio, Omar Gallo and Paul Velarde, students of the Faculty of Geology, Mining, Petroleum and Environmental Engineering (FIGEMPA) of the Universidad Central de Ecuador, who helped to install the equipment in 2019, and helped with the monitoring of the field sites. We acknowledge the authorities of the Universidad Central de Ecuador, the Research Direction (Direccion de Investigacion, Dr. B. Estrella), and the coordinator of the ARES AI programme (Dr. R. Saenz) for facilitating the research activities of Ilia Alomia during the elaboration of her PhD programme. The local Government of Santa Cruz, the team of Galápagos National Park (E. Vera, S. Bayas) and the Biosecurity Agency of Galaápagos helped us with the permissions to work in Galapagos. Sebastian Paez-Bimos provided support with the R scripts to process the data.

## Appendix A. Supplementary data

The supplementary materials contain information on the $^{40}Ar/^{39}Ar$ ages of the rock samples, and the volumetric water content ($m^3.m^{-3}$, mean ± 1 SD) at different matric potentials.

## References

Adelinet, M., Fortin, J., d'Ozouville, N., Violette, S., 2008. The relationship between hydrodynamic properties and weathering of soils derived from volcanic rocks, Galapagos Islands (Ecuador). Environ. Geol. 56, 45–58. https://doi.org/10.1007/s00254-007-1138-3.

Alomia Herrera, I., Paque, R., Maertens, M., Vanacker, V., 2022. History of land cover change in Santa Cruz Island, Galapagos. Land 11, 1017. https://doi.org/10.3390/LAND11071017.

Anindita, S., Sleutel, S., Vandenberghe, D., De Grave, J., Vandenhende, V., Finke, P., 2022. Land use impacts on weathering, soil properties, and carbon storage in wet Andosols, Indonesia. Geoderma 423, 115963. https://doi.org/10.1016/J.GEODERMA.2022.115963.

Barrera, V., Escudero, L., Valverde, M., Allauca, J., 2019. Productividad y sostenibilidad de los sistemas de producción agropecuaria de las islas Galápagos-Ecuador. Instituto Nacional de Investigaciones Agropecuarias de Ecuador, Quito, Ecuador.

Black, J., 1973. Galápagos, Archipiélago del Ecuador, 1st ed. Imprenta Europa, Quito, Ecuador., p. 138

Bow, C.S., 1979. Geology and Petrogeneses of the Lavas of Floreana and Santa Cruz Islands: Galapagos Archipelago. PhD thesis. University of Oregon, Eugene, US.

Buck, L.E., Lassoie, J.P., Fernandes, E.C.M., 1999. Agroforestry in Sustainable Agricultural Systems, 1st ed. CRC Press L.L.C, Boca Raton, US.

Buma, B., Gordon, D.R., Kleisner, K.M., Bartuska, A., Bidlack, A., DeFries, R., Ellis, P., Friedlingstein, P., Metzger, S., Morgan, G., Novick, K., Sanchirico, J.N., Collins, J.R., Eagle, A.J., Fujita, R., Holst, E., Lavallee, J.M., Lubowski, R.N., Melikov, C., Moore, L.A., Oldfield, E.E., Paltseva, J., Raffeld, A.M., Randazzo, N.A., Schneider, C., Uludere Aragon, N., Hamburg, S.P., 2024. Expert review of the science underlying nature-based climate solutions. Nat. Clim. Chang. 14, 402–406. https://doi.org/10.1038/s41558-024-01960-0.

Burbano, D.V., Valdivieso, J.C., Izurieta, J.C., Meredith, T.C., Ferri, D.Q., 2022. "Rethink and reset" tourism in the Galapagos Islands: Stakeholders' views on the sustainability of tourism development. Ann. Tour. Res. Empir. Insights 3, 100057. https://doi.org/10.1016/J.ANNALE.2022.100057.

Campbell, G.S., Norman, J.M., 1998. Heat Flow in the Soil. In: Campbell, G.S., Norman, J.M. (Eds.), An Introduction to Environmental Biophysics. Springer New York, New York, pp. 113–128. https://doi.org/10.1007/978-1-4612-1626-1_8.

Candra, N.I., Gerzabek, M.H., Ottner, F., Wriessnig, K., Tintner, J., Schmidt, G., Rechberger, M.V., Rampazzo, N., Zehetner, F., 2021. Soil development and mineral transformations along a one-million-year chronosequence on the Galápagos Islands. Soil Sci. Soc. Am. J. 85, 2077–2099. https://doi.org/10.1002/SAJ2.20317.

Carter, M.R., Gregorich, E.G., 2007. Soil Sampling and Methods of Analysis, 2nd ed. CRC Press, Boca Raton, US. https://doi.org/10.1201/9781420005.

Cusack, D.F., Chadwick, O.A., Hockaday, W.C., Vitousek, P.M., 2012. Mineralogical controls on soil black carbon preservation. Global Biogeochem. Cycles 26, GB2019. https://doi.org/10.1029/2011GB004109.

Davila, F., Bourke, R.M., McWilliam, A., Crimp, S., Robins, L., van Wensveen, M., Alders, R.G., Butler, J.R.A., 2021. COVID-19 and food systems in Pacific Island Countries, Papua New Guinea, and Timor-Leste: opportunities for actions towards

the sustainable development goals. Agric. Syst. 191, 103137. https://doi.org/10.1016/J.AGSY.2021.103137.
Dinter, T.C., Gerzabek, M.H., Puschenreiter, M., Strobel, B.W., Strahlhofer, M., Couenberg, P.M., Zehetner, F., 2020. Changes in topsoil characteristics with climate and island age in the agricultural zones of the Galapagos. Geoderma 376, 114534. https://doi.org/10.1016/j.geoderma.2020.114534.
Fox, J.M., McPhie, J., Carey, R.J., Jourdan, F., Miggins, D.P., 2021. Construction of an intraplate island volcano: the volcanic history of Heard Island. Bull. Volcanol. 83, 37. https://doi.org/10.1007/s00445-021-01452-5.
Ghuman, B.S., Lal, R., 1987. Effects of partial clearing on microclimate in a humid tropical forest. Agric. For. Meteorol. 40, 17–29. https://doi.org/10.1016/0168-1923(87)90051-7.
Gomes, L. de C., Cardoso, I.M., Mendonça, E. de S., Fernandes, R.B.A., Lopes, V.S., Oliveira, T.S., 2016. Trees modify the dynamics of soil CO2 efflux in coffee agroforestry systems. Agric. For. Meteorol. 224, 30–39. https://doi.org/10.1016/J.AGRFORMET.2016.05.001.
González, J.A., Montes, C., Rodriguez, J., Tapia, W., 2008. Rethinking the Galapagos Islands as a complex social-ecological system: Implications for conservation and management. Ecol. Soc. 13(2). https://doi.org/10.5751/ES-02557-130213.
Grothe, P.R., Cobb, K.M., Liguori, G., Di Lorenzo, E., Capotondi, A., Lu, Y., Cheng, H., Edwards, R.L., Southon, J.R., Santos, G.M., Deocampo, D.M., Lynch-Stieglitz, J., Chen, T., Sayani, H.R., Thompson, D.M., Conroy, J.L., Moore, A.L., Townsend, K., Hagos, M., O'Connor, G., Toth, L.T., 2020. Enhanced El Niño–Southern oscillation variability in recent decades. Geophys. Res. Lett. 47, e2019GL083906. https://doi.org/10.1029/2019GL083906.
von Haden, A.C., Marín-Spiotta, E., Jackson, R.D., Kucharik, C.J., 2019. Soil microclimates influence annual carbon loss via heterotrophic soil respiration in maize and switchgrass bioenergy cropping systems. Agric. For. Meteorol. 279, 107731. https://doi.org/10.1016/j.agrformet.2019.107731.
Hardwick, S.R., Toumi, R., Pfeifer, M., Turner, E.C., Nilus, R., Ewers, R.M., 2015. The relationship between leaf area index and microclimate in tropical forest and oil palm plantation: Forest disturbance drives changes in microclimate. Agric. For. Meteorol. 201, 187–195. https://doi.org/10.1016/J.AGRFORMET.2014.11.010.
Hart, T., Drew, E., Yeo, S., Almaraz, M., Beillouin, D., Cardinael, R., Garcia, E., Kay, S., Lovell, S.T., Rosenstock, T.S., Sprenkle-Hyppolite, S., Stolle, F., Suber, M., Thapa, B., Wood, S., Cook-Patton, S.C., 2023. Priority science can accelerate agroforestry as a natural climate solution. Nat. Clim. Chang. 13, 1179–1190. https://doi.org/10.1038/s41558-023-01810-5.
Instituto Nacional de Estadísticas y Censos, 2015. Análisis de resultados definitivos Censo de Población y Vivienda Galápagos. Instituto Nacional de Estadísticas y Censos, Quito, Ecuador, p. 46.
Iseman, T., Miralles-Wilhelm, F., 2021. Nature-Based Solutions in Agriculture the Case and Pathway for Adoption. Food and Agriculture Organization and The Nature Conservancy, Virginia, US. https://doi.org/10.4060/cb3141en.
Jäger, H., Kowarik, I., Tye, A., 2009. Destruction without extinction: long-term impacts of an invasive tree species on Galápagos highland vegetation. J. Ecol. 97, 1252–1263. https://doi.org/10.1111/j.1365-2745.2009.01578.x.
Jäger, H., San-José, M., Peabody, C., Chango, R., Sevilla, C., 2024. Restoring the threatened Scalesia forest: insights from a decade of invasive plant management in Galapagos. Front. For. Glob. Chang. 7, 1350498. https://doi.org/10.3389/FFGC.2024.1350498/BIBTEX.
Koga, N., Shimoda, S., Shirato, Y., Kusaba, T., Shima, T., Niimi, H., Yamane, T., Wakabayashi, K., Niwa, K., Kohyama, K., Obara, H., Takata, Y., Kanda, T., Inoue, H., Ishizuka, S., Kaneko, S., Tsuruta, K., Hashimoto, S., Shinomiya, Y., Aizawa, S., Ito, E., Hashimoto, T., Morishita, T., Noguchi, K., Ono, K., Katayanagi, N., Atsumi, K., 2020. Assessing changes in soil carbon stocks after land use conversion from forest land to agricultural land in Japan. Geoderma 377, 114487. https://doi.org/10.1016/J.GEODERMA.2020.114487.
Kutílek, M., Nielsen, D.R., 2015. Soil the Skin of the Planet Earth, 1st ed. Springer Science +Business Media, London.
Lal, R., 2016. Encyclopedia of Soil Science, 3rd ed. CRC Press, Boca Raton, US.
Lal, R., Cummings, D.J., 1979. Clearing a tropical forest I. Effects on soil and micro-climate. F. Crop. Res. 2, 91–107. https://doi.org/10.1016/0378-4290(79)90012-1.
Laruelle, J., 1966. Study of a Soil Sequence on Indefatigable Island. In: Bowman, R.I. (Ed.), The Galápagos. University of California Press, Berkeley, CA, USA, pp. 87–92.
Laruelle, J., Stoops, G., 1967. Minor elements in Galapagos soils. Pedologie 17, 232–257.
Lasso, L., Espinosa, J., 2018. Soils from the Galapagos Islands. In: Moreno, J., Espinosa, J., Bernal, G. (Eds.), The Soils of Ecuador. Springer International Publishing AG, Cham, pp. 139–150. https://doi.org/10.1007/978-3-319-25319-0_5.
Martins, da S., P.F, Cerri, C.C., Volkoff, B., Andreux, F., Chauvel, A., 1991. Consequences of clearing and tillage on the soil of a natural Amazonian ecosystem. For. Ecol. Manag. 38, 273–282. https://doi.org/10.1016/0378-1127(91)90148-O.
McBirney, A.R., Williams, H., 1969. Geology and Petrology of the Galápagos Islands. In: Geological Society of America Memoirs. Geological Society of America, pp. 1–197. https://doi.org/10.1130/MEM118-p1.
Mena, C.F., Paltán, H.A., Benitez, F.L., Sampedro, C., Valverde, M., 2020. Threats of climate Change in Small Oceanic Islands: The Case of climate and Agriculture in the Galapagos Islands, Ecuador. In: Walsh, S.J., Riveros-Iregui, D., Arce-Nazario, J., Page, P.H. (Eds.), Land Cover and Land Use Change on Islands. Social and Ecological Interactions in the Galapagos Islands. Springer, Cham, pp. 119–135. https://doi.org/10.1007/978-3-030-43973-6_5.
Mitchard, E.T.A., 2018. The tropical forest carbon cycle and climate change. Nature 559, 527–534. https://doi.org/10.1038/S41586-018-0300-2.
Molina, A., Vanacker, V., Corre, M.D., Veldkamp, E., 2019. Patterns in soil chemical weathering related to topographic gradients and vegetation structure in a high Andean tropical ecosystem. J. Geophys. Res. Earth Surf. 124, 666–685. https://doi.org/10.1029/2018jf004856.
Mu, Q., Heinsch, F.A., Zhao, M., Running, S.W., 2007. Development of a global evapotranspiration algorithm based on MODIS and global meteorology data. Remote Sens. Environ. 111, 519–536. https://doi.org/10.1016/j.rse.2007.04.015.
Nuruddin, A.A., Tokiman, L., 2005. Air and soil temperature characteristics of two sizes forest gap in tropical forest. Asian J. Plant Sci. 4, 144–148. https://doi.org/10.3923/ajps.2005.144.148.
Ochsner, T., 2019. Rain or Shine an Introduction to Soil Physical Properties and Processes, 2nd ed. Oklahoma State University Libraries, Stillwater. https://doi.org/10.22488/OKSTATE.21.000000.
Osher, L.J., Matson, P.A., Amundson, R., 2003. Effect of land use change on soil carbon in Hawaii. Biogeochemistry 65, 213–232. https://doi.org/10.1023/A:1026048612540.
Osman, K.T., 2013. Soils Principles, Properties and Management, 1st ed. Springer Science +Business Media Dordrecht, London. https://doi.org/10.1007/978-94-007-5663-2.
Otsuki, K., Yamanaka, N., Du, S., 2014. Vegetation Restoration on Loess Plateau. In: Tsunekawa, Atsushi, Liu, G., Yamanaka, N., Du, S. (Eds.), Restoration and Development of the Degraded Loess Plateau, China. Springer Tokyo, Tokio, pp. 233–254. https://doi.org/10.1007/978-4-431-54481-4.
Paltán, H.A., Benitez, F.L., Rosero, P., Escobar-Camacho, D., Cuesta, F., Mena, C.F., 2021. Climate and sea surface trends in the Galapagos Islands. Sci. Rep. 11, 14465. https://doi.org/10.1038/s41598-021-93870-w.
Páez-Bimos, S., Villacís, M., Morales, O., Calispa, M., Molina, A., Salgado, S., de Bievre, B., Delmelle, P., Muñoz, T., Vanacker, V., 2022. Vegetation effects on soil pore structure and hydraulic properties in volcanic ash soils of the high Andes. Hydrol. Processes 36 (9), e14678. https://doi.org/10.1002/hyp.14678.
Paltán, H.A., Benítez, F.L., Narvaez, M., Mateus, C., Mena, C.F., 2023. Water security and agricultural systems in the Galapagos Islands: vulnerabilities under uncertain future climate and land use pathways. Front. Water 5, 1245207. https://doi.org/10.3389/FRWA.2023.1245207/BIBTEX.
Paque, R., Alomia Herrera, I., Dixon, J.L., Molina, A., Zehetner, F., Vanacker, V., 2024. Constraining the effect of climate and rock porosity on weathering extent in the volcanic island of Santa Cruz (Galápagos, Ecuador). J. Geophys. Res.: Earth Surf. 129, e2024JF007651. https://doi.org/10.1029/2024JF007651.
Poeplau, C., Vos, C., Don, A., 2017. Soil organic carbon stocks are systematically overestimated by misuse of the parameters bulk density and rock fragment content. Soil 3, 61–66. https://doi.org/10.5194/soil-3-61-2017.
Pohlert, T., 2021. Type Package Title Calculate Pairwise Multiple Comparisons of Mean Rank Sums Extended.
Pryet, A., Domínguez, C., Tomai, P.F., Chaumont, C., d'Ozouville, N., Villacís, M., Violette, S., 2012. Quantification of cloud water interception along the windward slope of Santa Cruz Island, Galapagos (Ecuador). Agric. For. Meteorol. 161, 94–106. https://doi.org/10.1016/j.agrformet.2012.03.018.
R Core Team, 2022. R: The R Project for Statistical Computing [WWW Document]. R version 4.1.3. URL. https://www.r-project.org/ (accessed 3.29.22).
Rial, M., Martínez Cortizas, A., Taboada, T., Rodríguez-Lado, L., 2017. Soil organic carbon stocks in Santa Cruz Island, Galapagos, under different climate change scenarios. Catena 156, 74–81. https://doi.org/10.1016/j.catena.2017.03.020.
Robertson, E.C., Peck, D.L., 1974. Thermal conductivity of vesicular basalt from Hawaii. J. Geophys. Res. 79, 4875–4888. https://doi.org/10.1029/JB079I032P04875.
Rodríguez Rodríguez, A., Arbelo, C.D., Guerra, J.A., Mora, J.L., Armas, C.M., 2005. Organic Carbon in Forest Andosols of the Canary Islands and Effects of deforestation on Carbon losses by Water Erosion. In: Roose, E.J., Lal, R., Feller, C., Barthes, B., Stewart, B.A. (Eds.), Soil Erosion and Carbon Dynamics. CRC Press, Boca Raton, pp. 73–86. https://doi.org/10.1201/9780203491935-8.
Sampedro, C., Pizzitutti, F., Quiroga, D., Walsh, S.J., Mena, C.F., 2020. Food supply system dynamics in the Galapagos Islands: Agriculture, livestock and imports. Renew. Agric. Food Syst. 35, 234–248. https://doi.org/10.1017/S1742170518000534.
Schwartz, D., 2014. Volcanic, Structural, and Morphological History of Santa Cruz Island, Galápagos Archipelago. University of Idaho, Arctic.
Schwartz, D.M., Harpp, K., Kurz, M.D., Wilson, E., Van Kirk, R., 2022. Low-volume magmatism linked to flank deformation on Isla Santa Cruz, Galápagos Archipelago, using cosmogenic $^{3}$He exposure and $^{40}$Ar/$^{39}$Ar dating of fault scarps and lavas. Bull. Volcanol. 84, 82. https://doi.org/10.1007/s00445-022-01575-3.
Shukla, M.K., 2014. Soil Physics: An Introduction, 1st ed. CRC Press, Boca Raton, US.
Sobotkova, M., Snehota, M., Dohnal, M., Ray, C., 2011. Determination of hydraulic properties of a tropical soil of Hawaii using column experiments and inverse modeling. Rev. Bras. Ciência do Solo 35, 1229–1239. https://doi.org/10.1590/S0100-06832011000400016.
Sonneveld, B.G.J.S., Merbis, M.D., Arnal, M.F., 2018. Nature-Based Solutions for Agricultural Water Management and Food Security food and Agriculture Organization of the United Nations.
Sterling, S.M., Ducharne, A., Polcher, J., 2013. The impact of global land-cover change on the terrestrial water cycle. Nat. Clim. Chang. 3, 385–390. https://doi.org/10.1038/nclimate1690.
Stoops, G., 2014. Soils and Paleosoils of the Galápagos Islands: what we know and what we don't know, a meta-analysis. Pac. Sci. 68, 1–17. https://doi.org/10.2984/68.1.1.
Taboada, T., Rodríguez-Lado, L., Ferro-Vázquez, C., Stoops, G., Martínez Cortizas, A., 2016. Chemical Weathering in the Volcanic Soils of Isla Santa Cruz (Galápagos Islands, Ecuador). Geoderma 261, 160–168. https://doi.org/10.1016/j.geoderma.2015.07.019.
Taiyun, W., Simko, V., 2021. R Package "Corrplot": Visualization of a Correlation Matrix. (Version 0.92).
Toohey, R.C., Boll, J., Brooks, E.S., Jones, J.R., 2018. Effects of land use on soil properties and hydrological processes at the point, plot, and catchment scale in volcanic soils

near Turrialba, Costa Rica. Geoderma 315, 138–148. https://doi.org/10.1016/J.GEODERMA.2017.11.044.
Trueman, M., d'Ozouville, N., 2010. Characterizing the Galapagos terrestrial climate in the face of global climate change. Galapagos Res. 67, 26–37.
Trueman, M., Hannah, L., d'Ozouville, N., 2011. Terrestrial ecosystems in Galápagos: Potential responses to climate change. In: Larrea, I., Di Carlo, G. (Eds.), Climate Change Vulnerability Assessment of the Galápagos Islands of the Galápagos Islands. WWF and Conservation International, Quito, pp. 29–47.
USDA - NRCS, 2014. Claves para la Taxonomía de Suelos. Décima segunda Edición, 2014. USDA-NRCS.
Walsh, S.J., Mena, C.F., 2016. Interactions of social, terrestrial, and marine sub-systems in the Galapagos Islands, Ecuador. Proc. Natl. Acad. Sci. 113, 14536–14543. https://doi.org/10.1073/pnas.1604990113.
White, W.M., McBirney, A.R., Duncan, R.A., 1993. Petrology and geochemistry of the Galapagos Islands: portrait of a pathological mantle plume. J. Geophys. Res. 98. https://doi.org/10.1029/93jb02018.
Wickham, H., Averick, M., Bryan, J., Chang, W., D'Agostino Mcgowan, L., François, R., Grolemund, G., Hayes, A., Henry, L., Hester, J., Kuhn, M., Lin Pedersen, T., Miller, E., Bache, S.M., Müller, K., Ooms, J., Robinson, D., Seidel, D.P., Spinu, V., Takahashi, K., Vaughan, D., Wilke, C., Woo, K., Yutani, H., 2019. Welcome to the Tidyverse. J. Open Source Softw. 4, 1686. https://doi.org/10.21105/JOSS.01686.
World Metereological Organization (WMO), 2018. Guía de prácticas climatológicas, 2018th ed. Organización Meteorológica Mundial (OMM), Geneva, Switzerland.
Zheng, D., Hunt, E.R., Running, S.W., 1993. A daily soil temperature model based on air temperature and precipitation for continental applications. Clim. Res. 2, 183–191. https://doi.org/10.3354/cr002183.

## Further reading

Vanacker, V., Molina, A., Rosas, M.A., Bonnesoeur, V., Román-Dañobeytia, F., Ochoa-Tocachi, B.F., Buytaert, W., 2022. The effect of natural infrastructure on water erosion mitigation in the Andes. Soil 8, 133–147. https://doi.org/10.5194/soil-8-133-2022.